Opto-Electronics Review

journal homepage: https://journals.pan.pl/opelre

Optical and energy properties of $CdSe_{1-x}S_x$ thin films obtained by the method of high-frequency magnetron sputtering

Andrii Kashuba[1*], Bohdan Andriyevsky[2], Hryhorii Ilchuk[1], Ihor Semkiv[1], Ludmila Andriyevska[3], Iryna Moroz[1]

[1] Department of General Physics, Lviv Polytechnic National University, 12 Stepan Bandera St., Lviv, 79013, Ukraine
[2] Faculty of Electronics and Computer Sciences, Koszalin University of Technology, ul. Śniadeckich 2, 75-453 Koszalin, Poland
[3] Faculty of Civil Engineering, Environmental and Geodetic Sciences, Koszalin University of Technology, ul. Śniadeckich 2, 75-453 Koszalin, Poland

Article info

Article history:
Received 03 Oct. 2024
Received in revised form 16 Dec. 2024
Accepted 22 Dec. 2024
Available on-line 04 Feb. 2025

Keywords:
thin film;
optical transmission;
band gap;
bowing parameter;
spin-orbit splitting.

Abstract

$CdSe_{1-x}S_x$ ($x = 0$, 0.3, 0.4, 0.6, and 1) thin films were deposited on a quartz and silicon substrate using high-frequency magnetron sputtering. X-ray diffraction analysis estimated that the $CdSe_{1-x}S_x$ thin films are crystallized in a hexagonal structure [structure type – ZnO, space group $P6_3mc$ (No. 186)]. Spectral dependence of the optical transmittance between 300 and 1500 nm of the obtained thin films at room temperature was measured. Normalized integral optical transmittance, optical band gap, spin-orbit splitting, and the value of the bowing parameter of the $CdSe_{1-x}S_x$ thin films are determined. The values of the optical band gaps for $CdSe_{1-x}S_x$ thin films were estimated using the two methods (by Tauc plot and $dT/d\lambda$). Concentration dependences of the energy gaps connected with the leading optical transitions in $CdSe_{1-x}S_x$ (Γ_8^v–Γ_6^c, Γ_7^v–Γ_6^c) and spin-orbit splitting are studied. It is shown that the concentration dependences of main optical transitions are quadratic. The principal explanation for this seems to be the Burstein–Moss effect, which is caused by the doping atoms' excess carriers (electrons and holes).

1. Introduction

One of the perspective materials used for application in solar cells are cadmium chalcogenides (CdTe, CdSe, and CdS) thin films [1–3]. Usually, solar cells are constructed in a 'sandwich' form [4]. Such forms have active elements as transparent front contact, light-absorbing layer, window layer, and back contact [4]. Usually, for the light-absorbing layer cadmium telluride is used and for the window layer – cadmium sulfide (CdS/CdTe heterojunctions) [3]. As is well known, CdTe was crystallized in a cubic crystal structure [5] and CdS in a hexagonal one [6]. Lattice incoherence between CdTe and CdS layers can cause a photocurrent occurrence, negatively affecting the work of the solar cell. The formation of CdTe-CdS solid solutions between these layers reduces the lattice incoherence, but a high defect density causes a loss of efficiency [7]. CdSe can be an alternative solution to the problems originating from the CdTe/CdS junction [8, 9]. Using the cadmium selenide in solar cells can enhance the short circuit current density (J_{sc}) [10–14], but the open circuit voltage (V_{OC}) and fill factor (FF) decrease [10–12]. Using a CdS/CdSe as a window layer can enhance J_{sc} and maintain V_{OC}, thus improving device efficiency [10]. As a result, the optical and energy parameters of the $CdSe_{1-x}S_x$ thin films still need to be studied.

Previously, the authors reported on the synthesis and crystal structure of the $CdSe_{1-x}S_x$ thin film using the high-frequency (HF) magnetron sputtering method [15]. Here, the authors present the results of the experimental estimate of the leading optical properties of $CdSe_{1-x}S_x$ thin films deposited by HF magnetron sputtering.

2. Details of experiment

$CdSe_{1-x}S_x$ ($x = 0$, 0.3, 0.4, 0.6, and 1) thin films were deposited on quartz and silicon substrates ($16 \times 8 \times 1.1$ mm^3) by the HF magnetron sputtering (13.6 MHz) using a VUP-5M vacuum station (Selmi, Ukraine). Details of the thin-film deposition condition and crystal structure were reported

*Corresponding author at: andrii.i.kashuba@lpnu.ua

https://doi.org/10.24425/opelre.2025.153808
1896-3757/ Association of Polish Electrical Engineers (SEP) and Polish Academic of Sciences (PAS). Published by PAS

in [15] and some data from these measurements are listed in the Supplementary file. The spectral dependence of the optical transmittance of the obtained samples in the visible and near-infrared regions is studied at room temperature using a Shimadzu UV-3600 spectrometer.

3. Results and discussion

The spectral behaviour of the optical transmission of the $CdSe_{1-x}S_x$ thin-film-substrate (quartz) system is shown in Fig. 1(a). A sharp increase in the transmission coefficient in the range of wavelengths from ~480 nm ($x = 1$) to ~760 nm ($x = 0$) can be observed. This growth is characteristic of the edge of fundamental absorption. Additionally, the optical spectra are highly influenced by the film structure, which is, in turn, shaped by the preparation method, film thickness, and deposition conditions. The transmission spectra of the thin films display periodic peaks due to interference effects. This highlights the high structural quality of the thin films.

The normalized integrated transmission was calculated by (1):

$$T_{\text{aver}} = \frac{1}{b-a}\int_a^b T \cdot d\lambda\,, \tag{1}$$

where T_{aver} is the average transmission [see Fig. 1(b)]. The concentration dependence of the integral transmission value is described by a parabolic dependence with an upward deviation from the linear one.

Various methods were employed to determine the optical band gaps of the semiconductor films. One is the Tauc method [see Fig. 2(a)]. This method is based on a dependence of $(\alpha \cdot h\nu)^2 = f(h\nu)$ [16]. Additionally, the optical band gap energy can be determined from the maximum position in the transmittance first derivative ($dT/d\lambda$). The estimated band gap values of the studied $CdTe_{1-x}Se_x$ thin films obtained by the two above-mentioned methods show a good correlation (see Table 1).

From Fig. 2(a), the value of the direct zone-zone optical transition (E_g^{dir}) was determined, and it is denoted as: Γ_8^v–Γ_6^c (E_g) [17, 18]. It should be noted that the spectra of the absorption coefficient in Tauc coordinates [see Fig. 2(a)] show a break in linear behaviour at energies higher than E_g. This can be attributed to another optical transition, which corresponds to Γ_7^v–Γ_6^c (E_{g2}) [17, 18]. To confirm this assumption, the method of the first derivative of optical transmission spectra was used [see Fig. 2(b)]. From the example shown in Fig. 2(b), an intense peak that corresponds to the E_g, and a second one, less intense one that corresponds to the optical E_{g2} can be observed. From the established optical transitions E_g and E_{g2}, it is easy to establish the amount of spin-orbit splitting ($E_{SO} = E_{g2} - E_g$). The values of the optical band gaps and spin-orbit splitting are listed in Table 1.

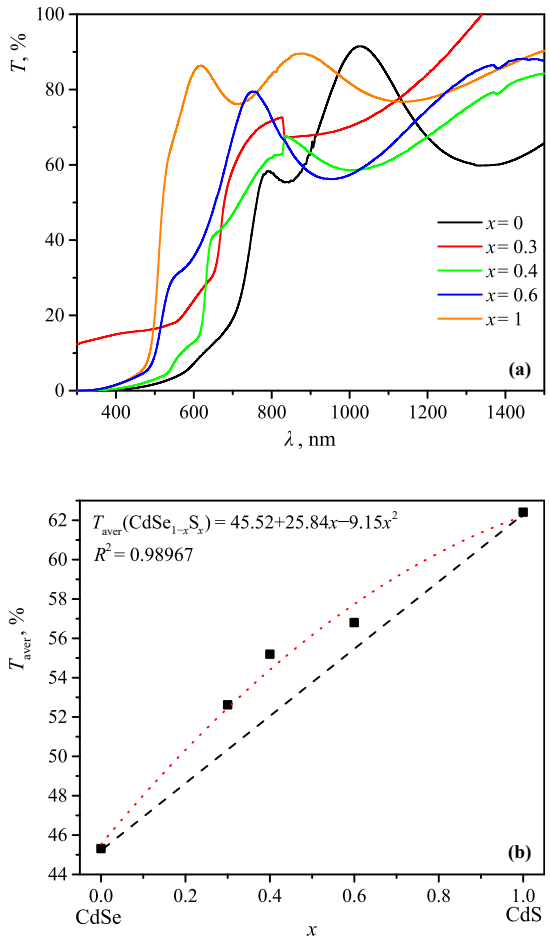

Fig. 1. Transmission spectra of a $CdSe_{1-x}S_x$ thin-film-substrate (quartz) system (a) and integral transmission of $CdSe_{1-x}S_x$ thin films for different S/Se composition ratios x (b).

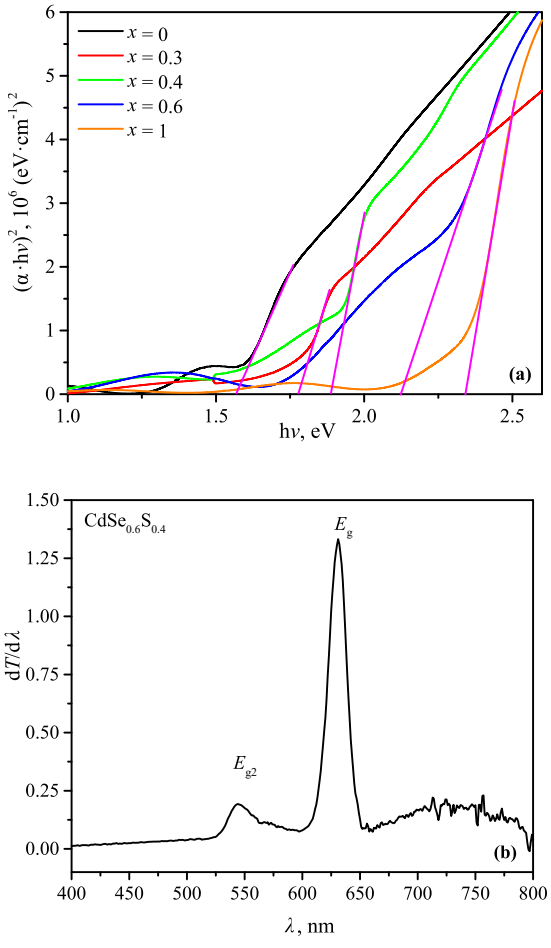

Fig. 2. Absorption spectra α in the presentation of $(\alpha \cdot h\nu)^2$ as a function of photon energy $h\nu$ (a) and wavelength spectrum of the transmittance derivative $dT/d\lambda$ (b) of $CdSe_{1-x}S_x$ thin films.

Table 1.
Energy properties of $CdSe_{1-x}S_x$ thin films obtained by HF magnetron sputtering.

x	E_g, eV (Tauc)	E_g, eV ($dT/d\lambda$)	E_{g2}, eV ($dT/d\lambda$)	E_{SO}, eV
0	1.60 ± 0.07	1.66 ± 0.10	2.04 ± 0.20	0.38 ± 0.02
0.3	1.77 ± 0.07	1.85 ± 0.11	2.14 ± 0.21	0.29 ± 0.02
0.4	1.89 ± 0.08	1.96 ± 0.12	2.28 ± 0.22	0.32 ± 0.02
0.6	2.17 ± 0.09	2.3 ± 0.14	2.46 ± 0.24	0.16 ± 0.01
1	2.34 ± 0.10	2.43 ± 0.15	2.48 ± 0.24	0.05 ± 0.003

Correlation analysis of the value of spin-orbit splitting with known literature data for a single crystal (see Table 2) indicates a decrease in the E_{SO} value when going from a single crystal sample (3D) to a thin film (2D). It can be assumed that this effect is associated with a decrease in the dispersion of energy levels in the thin film [18].

Table 2.
Comparative analysis of the value of spin-orbit splitting E_{SO} for $CdSe_{1-x}S_x$ thin films.

x	E_{SO} for thin films *from optical spectra* $P6_3mc$	x, [18]	E_{SO} for thin films *from DFT calculation* $P6_3mc$	x, [19]	E_{SO} for thin films *from optical spectra* $F\text{-}43m$	x, [20]	E_{SO} for single crystal *from optical spectra* $P6_3mc$
0	0.38 ± 0.02	0	0.29	0	0.30	0	0.42
0.3	0.29 ± 0.02	0.25	0.31	0.17	0.21	0.1	0.35
0.4	0.32 ± 0.02	0.50	0.29	0.35	0.21	0.4	0.31
0.6	0.16 ± 0.01	0.75	0.28	0.64	0.09	0.6	0.23
1	0.05 ± 0.003	1.00	0.28	1.00	–	1	0.07

The concentration dependences of the optical transitions E_g, E_{g2}, and the value of E_{SO} are presented in Fig. 3. These dependences are not linear, being rather described by quadratic functions [see the legends of Fig. 3 and (2)]. Deviation from linear dependence is a well-known phenomenon commonly observed in ternary alloy thin films. The main reason is the difference in lattice constants between the "parent" and their substitute atoms [17, 18].

$$E(x) = x \cdot E_{CdS} + (1-x) \cdot E_{CdSe} - \delta \cdot x \cdot (1-x), \qquad (2)$$

where δ is the bowing parameter. This bowing parameter can be decomposed into components [17, 18, 21]:

1) The component is related to the volume deformation effect, which is responsible for the change in the band gap of individual components of CdSe and CdS in a solid solution (δ_{VD}).
2) The component is related to the redistribution of charge between different bonds in the disordered solid solution (δ_{CE}).
3) The component describes the change in band gap upon relaxation of the positions of ions in the lattice of the solid solution (δ_{SR}).

$$\delta = \delta_{VD} + \delta_{CE} + \delta_{SR}. \qquad (3)$$

The value of the bowing parameter and its comparative analysis are given in Table 3. Attention should be paid to the sign of the bowing parameter, which is negative ($\delta < 0$). Similar behaviour of the bowing parameter was obtained for other solid solutions [22, 23]. The negative value of the bowing parameter means that the electron, excited from the valence band to the conduction band, should obtain a higher energy value than the band gap value. The manifestation of the Burstein can explain this phenomenon – Moss effect [24] which is associated with an excess of carriers (electrons and holes), which may originate from structural defects. These excess carriers lead to an increase in the band gap E_g.

Table 3.
Comparative analysis of the value of bowing parameter for $CdSe_{1-x}S_x$ thin films.

Sample	Crystal structure	Method or Ref.	δ for $E_g(\Gamma_8^v-\Gamma_6^c)$	δ for $E_{g2}(\Gamma_7^v-\Gamma_6^c)$
Thin film	$P6_3mc$	Tauc	−0.14	–
		$dT/d\lambda$	−0.24	−0.33
		GGA+PBEsol	0.13	0.12
Nanoparticle	$P6_3mc$	[19]	0.54	–
Thin film	$F\text{-}43m$	[17]	0.079	0.101
Crystal	$F\text{-}43m$	[25]	0.53, 0.54	–

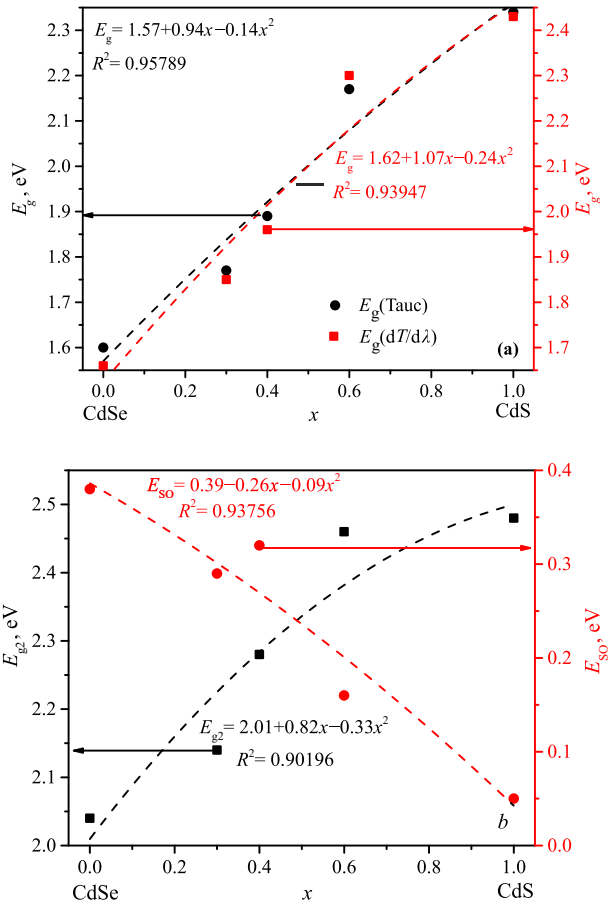

Fig. 3. Concentration dependences of the optical band gaps E_g (a), E_{g2}, and value of E_{SO} (b) for $CdSe_{1-x}S_x$ thin films.

For a more detailed analysis of the nature of deviation of the optical transitions E_g, E_{g2} from a linear dependence, the components of the bowing parameter should be determined. According to the method described in [21, 26], the parameters δ_{VD}, δ_{CE}, and δ_{SR} can be determined by (4)–(6), respectively:

$$\delta_{VD} = \frac{E^*_{CdS} - E_{CdS}}{1-x} + \frac{E^*_{CdSe} - E_{CdSe}}{x}, \quad (4)$$

$$\delta_{CE} = \frac{E_{CdS}}{1-x} + \frac{E_{CdSe}}{x} - \frac{E_{CdSe_{1-x}S_x}}{x(1-x)}, \quad (5)$$

$$\delta_{SR} = \frac{E_{CdSe_{1-x}S_x} - E^*_{CdSe_{1-x}S_x}}{x(1-x)}. \quad (6)$$

In (4)–(6), the top symbol (*) means the equilibrium energy of the alloy with the composition index x (the related data are indicated in the legends of Fig. 3). The determined values of the components of bowing parameter are given in Table 4.

Having obtained the components of the bowing parameter (see Table 4), it can be observed that a minor contribution to the bowing parameter is made by the component associated with the deflection due to the volume deformation effect (δ_{VD}). On the other hand, for $CdSe_{0.7}S_{0.3}$ and $CdSe_{0.6}S_{0.4}$ ($x < 0.5$) thin films, the determined contribution to the bowing parameter is the deflection coefficient which describes the change in the band gap upon relaxation of the ion positions in the solid solution lattice (δ_{SR}). However, in the $CdSe_{0.4}S_{0.6}$ thin film ($x > 0.5$), the bowing parameter is associated with the charge redistribution between different bonds in the disordered solid solution.

$CdSe_{1-x}S_x$ thin films have attracted significant interest in recent years [27–31]. Based on the information in [27–31], the authors can assume that the presented research results may have applications in photovoltaics. Specifically, these solid solutions of $CdSe_{1-x}S_x$ can form at the interface between the optical "window" (CdS or $CdSe_{1-x}S_x$ [27]) and the absorbing layer (CdTe or $CdSe_{1-x}Te_x$ [27]). Reference [32] reports the highest efficiencies of the (CdSe, CdTe)-junction solar cells at 26.55% and 23.69%, respectively. To achieve higher solar cell efficiency, one can choose compounds ($CdSe_{1-x}S_x$, $CdSe_{1-x}Te_x$)-crystalline alloy junction solar cells instead of (CdSe, CdTe)-junction solar cells [27]. In particular, Reference [27] demonstrates that the maximal efficiencies (34.375% (33.72%)) were obtained in $CdSe_{1-x}S_x$, $CdSe_{1-x}Te_x$-crystalline alloy junction solar cells at 300 K.

4. Conclusions

Optical spectra of the $CdSe_{1-x}S_x$ thin films deposited by HF magnetron sputtering were studied, as well as quartz and silicon were used as substrates for deposition films. The composition ratios of the thin films were established using the X-ray fluorescence spectroscopy (XRF) method ($CdSe_{0.7}Se_{0.3}$, $CdSe_{0.6}Se_{0.4}$, and $CdTe_{0.4}S_{0.6}$). X-ray diffraction (XRD) analysis estimated that the $CdSe_{1-x}S_x$ thin films are crystallized in a hexagonal structure. The spectral dependence of the optical transmittance between 300 and 1500 nm of the $CdSe_{0.7}Se_{0.3}$, $CdSe_{0.6}Se_{0.4}$ and $CdTe_{0.4}S_{0.6}$ thin films at room temperature was measured. The energy dependence of the optical absorption in the $(\alpha \cdot h\nu)^2 = f(h\nu)$ coordinate demonstrates the presence of the fundamental absorption edge with the band gap of a direct type for all studies of thin films. The values of the optical band gaps for $CdSe_{1-x}S_x$ ($x = 0 - 1$) thin films were also estimated using the $dT/d\lambda$. Both methods of the band gap estimation indicate good correlation and show an increase of the band gap with increasing of sulphur content in the thin films studied. An increasing character of the band gap dependence on the sulphur content $E_g(x)$ was found in the optical studies. The value of spin-orbital splitting for $CdSe_{1-x}S_x$ thin films was calculated based on the main optical energy transitions. A small deviation from the Vegard's law with bowing has been observed for the main optical transitions (Γ_8^v–Γ_6^c, Γ_7^v–Γ_6^c) and spin-orbital splitting. This deviation is mainly due to the relaxation of the ion positions in the solid solution lattice (δ_{SR}) for $x < 0.5$, and to the charge redistribution between different bonds in the disordered solid solution (δ_{CE}) for $x > 0.5$.

Table 4.
Components of the bowing parameter for $CdSe_{1-x}S_x$ thin films.

δ	Optical transition	$CdSe_{0.7}S_{0.3}$	$CdSe_{0.6}S_{0.4}$	$CdSe_{0.4}S_{0.6}$
δ_{VD}	E_g, eV (Tauc)	−0.057 ± 0.002	−0.025 ± 0.001	0.025 ± 0.001
	E_g, eV ($dT/d\lambda$)	−0.105 ± 0.006	−0.067 ± 0.004	−0.017 ± 0.001
	E_{g2}, eV ($dT/d\lambda$)	−0.071 ± 0.007	−0.042 ± 0.004	$-(3.7 \pm 0.2)\ 10^{-16}$
δ_{CE}	E_g, eV (Tauc)	0.248 ± 0.010	0.025 ± 0.001	−0.525 ± 0.022
	E_g, eV ($dT/d\lambda$)	0.195 ± 0.012	0.033 ± 0.002	−0.742 ± 0.045
	E_{g2}, eV ($dT/d\lambda$)	0.153 ± 0.015	−0.267 ± 0.026	−0.650 ± 0.064
δ_{SR}	E_g, eV (Tauc)	−0.331 ± 0.014	−0.140 ± 0.006	0.360 ± 0.015
	E_g, eV ($dT/d\lambda$)	−0.331 ± 0.020	−0.207 ± 0.013	0.518 ± 0.031
	E_{g2}, eV ($dT/d\lambda$)	−0.411 ± 0.040	−0.022 ± 0.002	0.320 ± 0.031

Acknowledgements

This research was supported by the National research foundation of Ukraine (project no. 2022.01/0163).

References

[1] Poplawsky, J. D. *et al*. Structural and compositional dependence of the $CdTe_xSe_{1-x}$ alloy layer photoactivity in CdTe-based solar cells. *Nat. Commun.* **7**, 12537 (2016). https://doi.org/10.1038/ncomms12537

[2] Bosio, A., Romeo, N., Mazzamuto, S. & Canevari, V. Polycrystalline CdTe thin films for photovoltaic applications. *Prog. Cryst. Growth Charact. Mater*. **52**, 247–279 (2006). https://doi.org/10.1016/j.pcrysgrow.2006.09.001

[3] Petrus, R. Yu. *et al*. Optical properties of materials for solar energy based on cadmium chalcogenides thin films. *Phys. Chem. Solid State* **20**, 367–371 (2019). https://doi.org/10.15330/pcss.20.4.367-371

[4] Romeo, N., Bosio, A., Mazzamuto, S., Romeo, A. & Vaillant-Roca, L. High Efficiency CdTe/CdS Thin Film Solar Cells with A Novel Back-Contact. in *22nd European Photovoltaic Solar Energy Conference* 1919–1921 (EU PVSEC, 2007).

[5] Kamel, N. S., Aadim, K. A. & Kadhim, A. Study of the characterizationn of CdTe thin films prepared by the pulsed laser deposition technique with different laser energies. *Adv. Nat. Sci: Nanosci. Nanotechnol*. **14**, 025015 (2023). https://doi.org/10.1088/2043-6262/acd683

[6] Wang, D., Li, X. & Qin, G. Relaxation effects on the structural and piezoelectric properties of wurtzite ZnS and CdS thin films under in-plane strain. *Microelectron. Eng.* **286**, 112131 (2024). https://doi.org/10.1016/j.mee.2023.112131

[7] Dumre, B. B. *et al*. Improved optoelectronic properties in $CdSe_xTe_{1-x}$ through controlled composition and short-range order. *Sol. Energy* **194**, 742–750 (2019). https://doi.org/10.1016/j.solener.2019.10.091

[8] Kashuba, A. I. *et al*. Growth, crystal structure and theoretical studies of energy and optical properties of $CdTe_{1-x}Se_x$ thin films. *Appl. Nanosci*. **12**, 335–342 (2022). https://doi.org/10.1007/s13204-020-01635-0

[9] Kashuba, A. I. & Andriyevsky, B. Growth and crystal structure of $CdTe_{1-x}Se_x$ ($x \geq 0.75$) thin films prepared by the method of high-frequency magnetron sputtering. *Low Temp. Phys*. **50**, 29–33 (2024). https://doi.org/10.1063/10.0023888

[10] Li, C. *et al*. Properties of $CdSe_{1-x}S_x$ films by magnetron sputtering and their role in CdTe solar cells. *J. Mater. Sci.: Mater. Electron*. **31**, 21455–21466 (2020). https://doi.org/10.1007/s10854-020-04659-y

[11] Paudel, N. R. & Yan, Y. Enhancing the photo-currents of CdTe thin-film solar cells in both short and long wavelength regions. *Appl. Phys. Lett*. **105**, 183510 (2014). https://doi.org/10.1063/1.4901532

[12] Baines, T. *et al*. Incorporation of CdSe layers into CdTe thin film solar cells. *Sol. Energy Mater. Sol. Cells*. **180**, 196–204 (2018). https://doi.org/10.1016/j.solmat.2018.03.010

[13] Bao, Z. *et al.* The study of CdSe thin film prepared by pulsed laser deposition for CdSe/CdTe solar cell. *J. Mater. Sci.: Mater. Electron*. **27**, 7233–7239 (2016). https://doi.org/10.1007/s10854-016-4689-9

[14] Bao, *Z. et al*. Synthesis and characterization of novel oxygenated CdSe window layer for CdTe thin film solar cells. *Mater. Sci. Semicond. Process*. **63**, 12–17 (2017). https://doi.org/10.1016/j.mssp.2017.01.003

[15] Kashuba, A., Semkiv, I., Andriyevsky, B., Ilchuk, H. & Pokladok, N. Structural and morphological properties of $CdSe_{1-x}S_x$ thin films obtained by the method of high-frequency magnetron sputtering. *Phys. Chem. Solid State* **25**, 40–44 (2024). https://doi.org/10.15330/pcss.25.1.40-44

[16] Tauc, J. Optical properties and electronic structure of amorphous Ge and Si. *Mater. Res. Bull.* **3**, 37–46 (1968). https://doi.org/10.1016/0025-5408(68)90023-8

[17] Zuala, L. & Agarwal, P. Effect of Se concentration on mixed phonon modes and spin orbit splitting in thermally evaporated CdS_xSe_{1-x} ($0 \leq x \leq 1$) films using CdS–CdSe nano-composites. *Mater. Chem. Phys*. **162**, 813–821 (2015). https://doi.org/10.1016/j.matchemphys.2015.07.008

[18] Kashuba, A. I. *et al.* Concentration dependences of electronic band structure of $CdSe_{1-x}S_x$ thin films. *Appl. Nanosci*. **13**, 4761–4770 (2023). https://doi.org/10.1007/s13204-022-02613-4

[19] Murphy, M. W. *et al*. Electronic structure and optical properties of CdS_xSe_{1-x} solid solution nanostructures from X-ray absorption near edge structure, X-ray excited optical luminescence, and density functional theory investigations. *J. Appl. Phys*. **166**, 193709 (2014). https://doi.org/10.1063/1.4902390

[20] Pedrotti, F. L. & Reynolds, D. C. Spin-orbit splitting in CdS:Se single crystals. *Phys. Rev.* **127**, 1584–1586 (1962). https://doi.org/10.1103/PhysRev.127.1584

[21] Ameri, M. *et al*. Structural and electronic properties calculations of $Be_xZn_{1-x}Se$ alloy. *Mater. Sci. Semicond. Process.* **10**, 6–13 (2007). https://doi.org/10.1016/j.mssp.2007.01.003

[22] Kim, K., Hart, G. L. W. & Zunger, A. Negative band gap bowing in epitaxial InAs/GaAs alloys and predicted band offsets of the strained binaries and alloys on various substrates. *Appl. Phys. Lett.* **80**, 3105–3107 (2002). https://doi.org/10.1063/1.1470693

[23] Singh, S. D. Determination of the optical gap bowing parameter for ternary $Ni_{1-x}Zn_xO$ cubic rocksalt solid solutions. *Dalton Trans.* **44**, 14793–14798 (2015). https://doi.org/10.1039/C5DT02283E

[24] Grundmann, M. *The Physics of Semiconductors. An Introduction Including Devices and Nanophysics*. (Springer, 2006). https://doi.org/10.1007/3-540-34661-9

[25] Hernandez-Calderon, I. Optical Properties and Electronic Structure of Wide Band Gap II–VI Semiconductors. in *II-VI Semiconductor Materials and their Applications* (Ed. Tamargo, M. C) 145 (Taylor and Francis, 2002).

[26] Bernard, J. E. & Zunger, A. Electronic structure of ZnS, ZnSe, ZnTe, and their pseudobinary alloys. *Phys. Rev. B* **36**, 3199–3228 (1987). https://doi.org/10.1103/PhysRevB.36.3199

[27] Van Cong, H. 34.375% (33.72%)-maximal efficiencies, obtained in $CdSe_{1-x}S_x$, $CdSe_{1-x}Te_x$-crystalline alloy junction solar cells at 300 K. *Eur. J. Appl. Sci. Eng. Technol*. **2**, 150–174 (2024). https://doi.org/10.59324/ejaset.2024.2(2).11

[28] Zafar, M. *et al*. *Ab initio* study of structural, electronic and elastic properties of $CdSe_{1-x}S_x$ semiconductor. *Sol. Energy* **158**, 63–70 (2017). https://doi.org/10.1016/j.solener.2017.09.034

[29] Lau, P. C., Zhu, Z., Norwood, R. A., Mansuripur, M. & Peyghambarian, N. Thermally robust and blinking suppressed core/graded-shell CdSe/CdSe1−xSx/CdS 'giant' multishell semiconductor nanocrystals. *Nanotechnology* **24**, 475705 (2013). https://doi.org/10.1088/0957-4484/24/47/475705

[30] Junda, M. M. *et al*. Optical Properties of $CdSe_{1-x}S_x$ and $CdSe_{1-y}Te_y$ Alloys and Their Application for CdTe Photovoltaics. in *2017 IEEE 44th Photovoltaic Specialist Conference (PVSC)* 3426–3429 (IEEE, 2017). https://doi.org/10.1109/PVSC.2017.8366483

[31] Almohammedi, A., Ashour, A. & Shaaban, E. R. Structural and optical investigations of chalcogenide $CdSe_{1-x}S_x$ thin films for optoelectronic applications. *Chalcogenide Lett*. **16**, 113–122 (2019). https://chalcogen.ro/113_AlmohammediA.pdf

[32] Van Cong, H. (14.82 %, 12.16 %, 26.55 %, or 23.69 %)-limiting highest efficiencies, respectively in n+(p+)−p(n) crystalline (X≡Ge,GaSb,CdTe, or CdSe)-junction solar cells, due to the effects of impurity size, temperature, heavy doping, and photovoltaic conversion. *SCIREA J. Phys.* **8**, 575–595 (2023). https://doi.org/10.54647/physics140591